Pergamon

Int. J. Solids Structures Vol. 33, No. 9, pp. 1287–1303, 1996
Copyright © 1996 Elsevier Science Ltd
Printed in Great Britain. All rights reserved
0020-7683/96 $15.00 + .00

0020-7683(95)00100-X

THE FINITE DEFORMATION OF NONLINEAR COMPOSITE MATERIALS—II. EVOLUTION OF THE MICROSTRUCTURE

M. ZAIDMAN and P. PONTE CASTAÑEDA
Department of Mechanical Engineering and Applied Mechanics, University of Pennsylvania, Philadelphia, PA 19104, U.S.A.

(*Received* 21 *September* 1994; *in revised form* 14 *April* 1995)

Abstract—This work deals with the development of constitutive models for two-phase nonlinearly viscous and rigid–perfectly plastic composites with evolving microstructures. Part I of the work was concerned with the estimation of instantaneous constitutive relations for the class of particulate microstructures with aligned ellipsoidal inclusions. This second part deals with the identification of appropriate variables characterizing the state of the microstructure, and with the development of evolution equations for these variables. Under the assumption of triaxial loading conditions, it is argued that aligned ellipsoidal inclusions deform—in some average sense—into ellipsoidal inclusions with different size and shape. The appropriate state variables are thus the current values of the volume fractions of the phases and the aspect ratios of the inclusions. The pertinent evolution laws then follow from well-known kinematical relations, together with appropriate estimates for the average strain rate in the inclusion and matrix phase. The resulting constitutive models take the form of standard homogenized stress–strain rate relations, supplemented by evolution equations for the above-mentioned state variables. Although the ultimate goal of this study is to be able to model complex forming processes, illustrative results are given here only for axisymmetric and plane strain deformations of composites with rigid–perfectly plastic phases. The main conclusion is that effective behavior of these composites will not be perfectly plastic, but may exhibit hardening, or even softening, depending on the specific nature of the applied loading conditions.

1. INTRODUCTION

In this paper, we continue the development of constitutive models for two-phase nonlinearly viscous and rigid–perfectly plastic composites with evolving microstructures. In Part I of this work (Ponte Castañeda and Zaidman, 1995), we obtained variational estimates for the instantaneous effective potentials and yield functions of power-law viscous and perfectly plastic composites, respectively, with particulate microstructures containing aligned ellipsoidal inclusions. In this second part, we address the problem of finding appropriate state variables serving to characterize the evolution of the microstructure. Under the assumption of triaxial loading conditions (with fixed axes), we argue that, on the average, the aligned ellipsoidal inclusions deform into aligned ellipsoidal inclusions of different size and shape, or equivalently, that the strain rate in the inclusions is uniform, again in some average sense. This suggests identifying the volume fractions of the phases and the aspect ratios of the inclusions in the instantaneous effective potentials of Part I with the relevant variables characterizing the state of the microstructure. Evolution laws can then be determined from standard kinematical equations relating the change in volume and shape of an ellipsoidal inclusion to the current value of the (average) strain rates in the inclusion, which in turn can be related to the average strain rate in the composite. These estimates for the average strain rates in the inclusion are obtained via the Hashin–Shtrikman variational principles of Willis (1977, 1978) for linearly viscous composites, and the results are extended for the nonlinearly viscous composites by means of the variational principles of Ponte Castañeda (1991, 1992). In summary, the constitutive model takes the form of the effective stress–strain rate relations of Part I, complemented by ordinary differential equations for the evolution of the volume fraction and aspect ratios of the inclusions.

The paper is structured as follows. Section 2 presents the general theory for linearly viscous composites with dilute and nondilute concentrations of aligned ellipsoidal inclusions. Special results are also given for incompressible viscous fluids. Section 3 deals

with the extension of the model to (incompressible) power-law viscous and rigid–perfectly plastic composites, for which instantaneous effective potentials are explicitly available from Part I. Section 4 is concerned with the application of the constitutive models to homogeneous axisymmetric deformations of both linearly viscous and rigid–perfectly plastic two-phase composites, and Section 5 presents some results for plane strain deformations of rigid–perfectly plastic two-phase composites. The main results are that the effective behavior of the composites with linearly viscous phases is in fact nonlinear, and analogously, that the effective behavior of the composites with perfectly plastic phases is not perfectly plastic, but may exhibit hardening, or even softening, as a direct consequence of the microstructure evolution.

2. LINEARLY VISCOUS COMPOSITES WITH EVOLVING MICROSTRUCTURES

As discussed in Part I of this work, Willis (1977, 1978) provided variational estimates of the Hashin–Shtrikman (1963) type for the effective properties of linearly viscous (analogous to linear elastic) two-phase composites with particulate microstructures exhibiting "ellipsoidal symmetry". This class of microstructures corresponds to aligned, self-similar ellipsoidal inclusions, with aspect ratios $w_1 = l_3/l_1$ and $w_2 = l_3/l_2$, distributed in a continuous matrix phase according to "stretched" statistically isotropic two-point correlation functions (see Fig. 1 of Part I). If we denote the proportions and viscosity tensors of the inclusion and matrix phases by $c^{(1)}$, $c^{(2)}$ and $\mathbf{L}^{(1)}$, $\mathbf{L}^{(2)}$, respectively, the effective viscous compliance tensor $\tilde{\mathbf{M}} = \tilde{\mathbf{L}}^{-1}$, relating the average strain rate $\bar{\mathbf{D}}$ to the average stress $\bar{\boldsymbol{\sigma}}$, may be expressed in the form

$$\tilde{\mathbf{M}} = \{\mathbf{I} + c^{(1)}[(\mathbf{M}^{(1)}\mathbf{L}^{(2)} - \mathbf{I})^{-1} + c^{(2)}(\mathbf{I} - \mathbf{S}^{(2)})]^{-1}\}\mathbf{M}^{(2)}, \tag{1}$$

where $\mathbf{S}^{(2)}$ denotes the Eshelby (1957) tensor associated with an ellipsoidal inclusion, with the given aspect ratios w_1 and w_2, embedded in a matrix of phase 2.

We recall that the above estimate for $\tilde{\mathbf{M}}$ was obtained via the Hashin–Shtrikman variational principles in terms of the average polarization fields, relative to a homogeneous comparison material, in the two phases of the composite. From these average polarization fields, it is straightforward to compute the average stress and strain rate fields in the two phases. For example, the average strain rate in the inclusions $\mathbf{D}^{(1)}$, which we will require later in this section, is given, in terms of the average strain intensity tensor $\mathbf{A}^{(1)}$, such that $\mathbf{D}^{(1)} = \mathbf{A}^{(1)}\bar{\mathbf{D}}$ (Hill, 1965), by

$$\mathbf{A}^{(1)} = [\mathbf{I} + c^{(2)}\mathbf{S}^{(2)}(\mathbf{M}^{(2)}\mathbf{L}^{(1)} - \mathbf{I})]^{-1}. \tag{2}$$

We emphasize that the above estimates for $\tilde{\mathbf{M}}$ and $\mathbf{A}^{(1)}$ are rigorously valid for all values of the concentration of the ellipsoidal inclusions (i.e. for $0 < c^{(1)} < 1$). In addition, it is useful to note that these estimates are in agreement with the well-known estimates of Eshelby (1957) for composites with dilute concentrations of inclusions (with $c^{(1)} \to 0$ and $c^{(2)} \to 1$). More generally, however, the above estimates for both $\tilde{\mathbf{M}}$ and $\mathbf{A}^{(1)}$ account for interaction effects through their dependence on the proportion of inclusions $c^{(1)}$ (or, equivalently, through $c^{(2)} = 1 - c^{(1)}$).

For composites with dilute concentrations of aligned ellipsoidal inclusions, Eshelby (1957) has also shown that the strain rate in the inclusions is itself uniform and therefore equal to its average, as determined by eqn (2) with $c^{(2)}$ set equal to 1. This result implies that an initially ellipsoidal inclusion will deform into ellipsoidal shapes with possibly different size, aspect ratios and orientations. It follows from this observation that the proportion of the phases satisfy the kinematical relations

$$\dot{c}^{(1)} = -\dot{c}^{(2)} = c^{(1)}c^{(2)}(\operatorname{tr}\mathbf{D}^{(1)} - \operatorname{tr}\mathbf{D}^{(2)}), \tag{3}$$

where $\mathbf{D}^{(2)}$ is the average strain rate in the matrix phase (such that the average strain rate

in the composite is given by $\bar{\mathbf{D}} = c^{(1)}\mathbf{D}^{(1)} + c^{(2)}\mathbf{D}^{(2)}$). In addition, it also follows that the aspect ratios of the self-similar ellipsoidal inclusions evolve according to the relations

$$\dot{w}_1 = (D_{33}^{(1)} - D_{11}^{(1)})w_1 \quad \text{and} \quad \dot{w}_2 = (D_{33}^{(1)} - D_{22}^{(1)})w_2. \tag{4}$$

Finally, expressions may also be obtained for the rate of rotation of the axes of the inclusion. However, in this work, we will restrict our attention to triaxial loading conditions, aligned with the principal axes of the ellipsoids, in such a way that the ellipsoids do not rotate.

Still within the context of composites with dilute concentrations of aligned inclusions, and for applied uniform velocity on the boundary, given by $\mathbf{v} = \bar{\mathbf{D}}\mathbf{x}$, the dilute version of relation (2) for the strain intensity tensor $\mathbf{A}^{(1)}$ permits the computation, via eqns (3) and (4), of the evolution of the volume fraction $c^{(1)}$ and aspect ratios w_1 and w_2 of the inclusions, respectively. If, on the other hand, uniform tractions, $\boldsymbol{\sigma}\mathbf{n} = \bar{\boldsymbol{\sigma}}\mathbf{n}$ (where $\mathbf{n}$ denotes the outward normal to the boundary of the composite), are prescribed on the boundary of the composite, the average strain rate may be computed from the effective relation $\bar{\mathbf{D}} = \tilde{\mathbf{M}}\bar{\boldsymbol{\sigma}}$, together with the dilute version of eqn (1). Once this is accomplished, we may proceed as in the previous case.

The application of Eshelby's procedure to compute the evolution of the aspect ratios of an isolated ellipsoidal inclusion of an incompressible viscous fluid, embedded in a matrix of another, has been considered by several authors, including Bilby *et al.* (1975) for the axisymmetric deformations of spheroidal inclusions and the planar deformation of elliptic cylinders, and Howard and Brierley (1976) for plane deformations of ellipsoidal inclusions. In addition, Bilby and Kolbuszewski (1977) have considered the rotation of elliptic cylinders and ellipsoids.

Ponte Castañeda and Zaidman (1994) argued, in the context of a linearly viscous porous material with a finite (nondilute) concentration of voids, subjected to triaxial loading conditions, that the initially spherical voids could still be assumed to deform, on the average, into ellipsoidal voids, aligned with the loading axes, with evolving volume and aspect ratios—exactly as for the case of porous materials with dilute volume fractions of pores, except that the finite volume fraction strain-rate intensity tensor, as obtained from the Hashin–Shtrikman variational principles, should be used instead of its dilute counterpart, as originally proposed by Eshelby. Clearly, the same assumption can be made if the inclusions are assumed to be linearly viscous instead of vacuous. Thus, in this work, we propose to make use of eqns (2), (3) and (4) to model approximately the evolution of the volume fraction and aspect ratios of the inclusions in a composite with finite concentrations of inclusions. The volume fraction and aspect ratios of the inclusions will be interpreted in this model as "internal variables" characterizing the state of the microstructure, under a given finite deformation history.

As discussed in Ponte Castañeda and Zaidman (1994), the main approximation involved in the adoption of the above model to account for the evolution of the microstructure in the two-phase composite with particulate microstructure is the fact that the microstructure of the composite is implicitly assumed to remain "ellipsoidal"—with the same aspect ratio for the distribution and shape of the inclusions (see Fig. 1 of Part I). This will clearly only be the case if the inclusions and the matrix are made of the same material, which is of course the trivial case. However, it is well known that the effect of inclusion distribution is of higher order, in the volume fraction of the inclusions, than the effect of inclusion shape on both the effective modulus tensor and on the strain intensity tensor [see Ponte Castañeda and Zaidman (1994, Section 3.3)]. Therefore, provided that the concentration of inclusions is not too high, the error introduced by the assumption that the microstructure evolves with the same aspect ratio for the distribution and shape of the inclusions should be small in relative terms. Improvements of the model would involve the introduction of a new internal variable characterizing the aspect ratio of the distribution of the inclusions, with a separate evolution equation for such a variable. Unfortunately, the required Hashin–Shtrikman estimates for such a model are not yet available.

The main goal, however, of the work of Ponte Castañeda and Zaidman (1994) was to provide a model for the effective behavior of nonlinearly viscous porous materials (including rigid–perfectly plastic composites) with evolving microstructures. The model was made possible by a consistent application of the nonlinear variational principles of Ponte Castañeda (1991, 1992) to estimate the average strain rate in the pores, as well as the effective potential of the nonlinearly viscous porous material in terms of corresponding information for linearly viscous porous materials, as just discussed. In this work, we attempt a similar analysis for two-phase nonlinearly viscous composites with incompressible phases. The determination of the effective potentials and yield functions for this class of composites was discussed in Part I of this work. In this part, we will make use of the above results for the evolution of the microstructure in two-phase linearly viscous composites (with finite concentrations of inclusions) to generate corresponding results for the evolution problem for two-phase nonlinearly viscous and rigid–perfectly plastic composites.

Before proceeding with the development of the model for the nonlinear composites, we specialize below the model for the linearly viscous composites to incompressible behavior for the two phases, with viscosities $\mu^{(1)}$ and $\mu^{(2)}$. In this case, the proportions of the two phases, $c^{(1)}$ and $c^{(2)}$, remain fixed due to incompressibility. On the other hand, for triaxial loading conditions, aligned with the axes of the deforming "ellipsoids", the aspect ratios evolve according to

$$\dot{w}_1 = w_1(A^{(1)}_{33ij} - A^{(1)}_{11ij})\bar{D}_{ij} \text{ and } \dot{w}_2 = w_2(A^{(1)}_{33ij} - A^{(1)}_{22ij})\bar{D}_{ij}, \tag{5}$$

where the strain rate intensity tensor, from eqn (2), may be rewritten in the form

$$\mathbf{A}^{(1)} = \mathbf{A}^{(1)}(y^{(1)}; w_1, w_2). \tag{6}$$

In this last relation, we recall that $y^{(1)} = \mu^{(2)}/\mu^{(1)}$, and we note that the explicit dependence on $c^{(1)}$ has been dropped because $c^{(1)}$ is fixed (although not necessarily infinitesimal). Equations (5), supplemented with eqn (6), are then to be solved together with

$$\bar{\mathbf{D}} = \tilde{\mathbf{M}}\bar{\boldsymbol{\sigma}}, \tag{7}$$

where, from eqn (1), $\tilde{\mathbf{M}}$ may be written in the form

$$\tilde{\mathbf{M}} = \frac{1}{3\mu^{(2)}}\tilde{\mathbf{m}}(y^{(1)}; w_1, w_2), \tag{8}$$

for the evolution of w_1, w_2, and $\bar{\boldsymbol{\sigma}}$ (if $\mathbf{v} = \bar{\mathbf{D}}\mathbf{x}$ is prescribed on the boundary) or $\bar{\mathbf{D}}$ (if $\boldsymbol{\sigma}\mathbf{n} = \bar{\boldsymbol{\sigma}}\mathbf{n}$ is prescribed on the boundary). We emphasize that uniform boundary conditions have been assumed for the purpose of carrying out the homogenization procedure, but once this is accomplished the above constitutive equations may be used for general boundary conditions, provided that the scale of variation of the applied loading conditions is large relative to the corresponding size of the typical inhomogeneity. For the case of nonuniform boundary conditions, however, the usual equilibrium and compatibility conditions for the average stress and strain rate, $\bar{\boldsymbol{\sigma}}$ and $\bar{\mathbf{D}}$, must be added to the homogenized constitutive relation. Note that the resulting homogenized constitutive model takes the usual form, but is complemented by evolution equations for the now position-dependent internal variables. For simplicity, in this work, we will only consider the case of uniform boundary conditions in Sections 4 and 5.

3. NONLINEARLY VISCOUS COMPOSITES WITH EVOLVING MICROSTRUCTURES

We recall, from Part I of this work, that the effective behavior of nonlinearly viscous composites with isotropic and incompressible phases is given by

$$\bar{\mathbf{D}} = \frac{\partial \tilde{U}}{\partial \bar{\boldsymbol{\sigma}}}(\bar{\boldsymbol{\sigma}}), \tag{9}$$

where $\tilde{U}$ is the effective strain rate potential. We also recall that we were able to derive estimates for the effective potentials $\tilde{U}$ of nonlinearly viscous composites with particulate microstructures, in terms of corresponding estimates for the effective viscous compliance tensors $\tilde{\mathbf{M}}$ of linearly viscous comparison composites with the same type of microstructures. This was accomplished by means of the variational procedure of Ponte Castañeda (1991, 1992), giving the following estimate for $\tilde{U}$:

$$\tilde{U}(\bar{\boldsymbol{\sigma}}) = \max_{\mu^{(1)},\mu^{(2)} \geqslant 0} \left\{ \frac{1}{2} \bar{\boldsymbol{\sigma}} \cdot (\tilde{\mathbf{M}} \bar{\boldsymbol{\sigma}}) - \sum_{r=1}^{2} c^{(r)} V^{(r)}(\mu^{(r)}) \right\}, \tag{10}$$

where the functions $V^{(r)}$ were defined in Part I. It follows from eqns (9) and (10) that the effective stress–strain rate relations for the nonlinearly viscous composites may be expressed in the form

$$\bar{\mathbf{D}} = \tilde{\mathbf{M}}(\hat{\mu}^{(1)}, \hat{\mu}^{(2)}) \bar{\boldsymbol{\sigma}}, \tag{11}$$

where $\hat{\mu}^{(1)} = \hat{\mu}^{(1)}(\bar{\boldsymbol{\sigma}})$ and $\hat{\mu}^{(2)} = \hat{\mu}^{(2)}(\bar{\boldsymbol{\sigma}})$ are the optimal values of $\mu^{(1)}$ and $\mu^{(2)}$ from the optimization problem (10) for $\tilde{U}$. We emphasize that, in spite of its appearance, the constitutive relation (11) is fully nonlinear, both directly through the dependence of $\hat{\mu}^{(1)}$ and $\hat{\mu}^{(2)}$ on $\bar{\boldsymbol{\sigma}}$, and indirectly through the dependence of $\hat{\mu}^{(1)}$ and $\hat{\mu}^{(2)}$ on the (changing) aspect ratios.

In addition, we note that the form (11) for the effective constitutive response suggests that the nonlinearly viscous composites may be thought of as linearly viscous composites with variable viscosities $\hat{\mu}^{(1)}$ and $\hat{\mu}^{(2)}$, depending on the current values of the average stress $\bar{\boldsymbol{\sigma}}$ and aspect ratios w_1 and w_2. In particular, this means that the average strain rate within the inclusions of the nonlinearly viscous composites may be estimated, at any given instant, from the relation $\mathbf{D}^{(1)} = \mathbf{A}^{(1)} \bar{\mathbf{D}}$, where $\mathbf{A}^{(1)}$ is the strain concentration tensor associated with $\tilde{\mathbf{M}}$, evaluated at the current values of $\hat{\mu}^{(1)}$ and $\hat{\mu}^{(2)}$ (and of w_1, w_2). Then, the evolution of the microstructure, for the nonlinearly viscous composites, may be treated in exactly the same way as that described in the previous section for the incompressible linearly viscous composites, except that the relevant phase "viscosities" $\hat{\mu}^{(1)}$ and $\hat{\mu}^{(2)}$ need now be taken to be dependent on $\bar{\boldsymbol{\sigma}}$ and w_1, w_2. Below we describe this procedure more explicitly in the context of the specific examples of power-law viscous and rigid–perfectly plastic composites with particulate microstructures.

For two-phase composites, with the inclusion and matrix phases in fixed proportions $c^{(1)}$ and $c^{(2)}$, respectively, and with pure power-law potentials

$$\phi^{(r)}(\sigma_e) = \frac{1}{3(n+1)\eta^{(r)}} \sigma_e^{n+1} = \frac{\sigma_y^{(r)}}{(n+1)} \left[\frac{\sigma_e}{\sigma_y^{(r)}} \right]^{n+1}, \tag{12}$$

where n (in the range $[1, \infty]$) and $\sigma_y^{(r)} = (3\eta^{(r)})^{1/n}$ are the power exponent and reference stress of phase r ($r = 1, 2$), the estimate (10) for the effective potential simplifies to

$$\tilde{U}(\bar{\boldsymbol{\sigma}}) = \frac{1}{(n+1)(\sigma_y^{(2)})^n} \max_{y^{(1)} \geqslant 0} \left\{ \frac{(\bar{\boldsymbol{\sigma}} \cdot [\tilde{\mathbf{m}}(y^{(1)}) \bar{\boldsymbol{\sigma}}])^{\frac{n+1}{2}}}{[c^{(2)} + c^{(1)} (z^{(2)})^{\frac{2n}{n-1}} (y^{(1)})^{\frac{n+1}{n-1}}]^{\frac{n-1}{2}}} \right\}, \tag{13}$$

where $y^{(1)} = \mu^{(2)}/\mu^{(1)}$, $z^{(2)} = \sigma_y^{(1)}/\sigma_y^{(2)}$ and $\tilde{\mathbf{m}} = 3\mu^{(2)}\tilde{\mathbf{M}}$ is the appropriately normalized estimate (1). We note that the optimal value of $y^{(1)}$, denoted $\hat{y}^{(1)}$, depends on the applied stress $\bar{\boldsymbol{\sigma}}$, the properties of the phases through the ratio $z^{(2)}$, and also on the state of the microstructure

through the current values of the aspect ratios w_1 and w_2. In addition, the corresponding effective stress–strain rate relations (11) reduce to

$$\bar{\mathbf{D}} = \frac{1}{(\sigma_y^{(2)})^n}\left[\frac{\bar{\boldsymbol{\sigma}}\cdot[\tilde{\mathbf{m}}(\hat{y}^{(1)})\bar{\boldsymbol{\sigma}}]}{c^{(2)}+c^{(1)}(z^{(2)})^{\frac{2n}{n-1}}(\hat{y}^{(1)})^{\frac{n+1}{n-1}}}\right]^{\frac{n-1}{2}}\tilde{\mathbf{m}}(\hat{y}^{(1)})\bar{\boldsymbol{\sigma}}. \tag{14}$$

Thus, the effective response of the power-law viscous composite, for a finite deformation program, is determined by relations (13) for the potential $\tilde{U}$ and (14) for the stress–strain rate relations, supplemented by relations (5) for the evolution of the aspect ratios of the inclusions w_1 and w_2, where $\mathbf{A}^{(1)}$ is obtained from relation (2) with

$$\mathbf{A}^{(1)} = \mathbf{A}^{(1)}(\hat{y}^{(1)}; w_1, w_2). \tag{15}$$

This expression evidently depends, through the ratio $\hat{y}^{(1)}$, on the average stress $\bar{\boldsymbol{\sigma}}$, on the state of the microstructure through the current values of w_1 and w_2, and also on the properties of the nonlinear phases through the ratio $z^{(2)}$. This demonstrates that, in general, the microstructure of the nonlinearly viscous composites will evolve differently from that of linearly viscous composites.

For the special case of a rigid–perfectly plastic composite, the expression (9) for the effective stress–strain rate relation is replaced by

$$\bar{\mathbf{D}} = \dot{\Lambda}\frac{\partial\tilde{\Phi}}{\partial\bar{\boldsymbol{\sigma}}}(\bar{\boldsymbol{\sigma}}), \tag{16}$$

where $\tilde{\Phi}(\bar{\boldsymbol{\sigma}}) = 0$ defines the effective yield surface of the composite, and may be estimated from (see Part I)

$$\tilde{\Phi}(\bar{\boldsymbol{\sigma}}) = \max_{y^{(1)}\geq 0}\{[c^{(2)}+c^{(1)}(z^{(2)})^2 y^{(1)}]^{-1}\bar{\boldsymbol{\sigma}}\cdot[\tilde{\mathbf{m}}(y^{(1)})\bar{\boldsymbol{\sigma}}]-(\sigma_y^{(2)})^2\}. \tag{17}$$

The evolution of the aspect ratios of the inclusions w_1 and w_2 is still determined by eqns (5), where $\mathbf{A}^{(1)}$ is given by eqn (15), in terms of the optimal value of $y^{(1)}$ from eqn (17). Finally, the plastic loading factor $\dot{\Lambda}$ may be obtained from the consistency condition requiring that

$$\dot{\tilde{\Phi}}(\bar{\boldsymbol{\sigma}}; w_1, w_2) = \frac{\partial\tilde{\Phi}}{\partial\bar{\sigma}_{ij}}\dot{\bar{\sigma}}_{ij}+\frac{\partial\tilde{\Phi}}{\partial w_1}\dot{w}_1+\frac{\partial\tilde{\Phi}}{\partial w_2}\dot{w}_2 = 0, \tag{18}$$

where we have not distinguished between the objective Jaumann and standard time derivative because, for triaxial loading conditions, the principal axes of the applied stress $\bar{\boldsymbol{\sigma}}$ do not rotate. The final result for the stress–strain rate relation may be written in the form

$$\bar{D}_{ij} = \frac{1}{H}\frac{\partial\tilde{\Phi}}{\partial\bar{\sigma}_{ij}}\frac{\partial\tilde{\Phi}}{\partial\bar{\sigma}_{kl}}\dot{\bar{\sigma}}_{kl}, \tag{19}$$

where H is the effective rate of hardening, given by

$$H = -\left[\left(w_1\frac{\partial\tilde{\Phi}}{\partial w_1}\right)(A_{33ij}^{(1)}-A_{11ij}^{(1)})\frac{\partial\tilde{\Phi}}{\partial\bar{\sigma}_{ij}}+\left(w_2\frac{\partial\tilde{\Phi}}{\partial w_2}\right)(A_{33ij}^{(1)}-A_{22ij}^{(1)})\frac{\partial\tilde{\Phi}}{\partial\bar{\sigma}_{ij}}\right]. \tag{20}$$

We emphasize that the effective hardening rate H is not zero in general, even though the constituent phases are perfectly plastic themselves. This is due to the fact that the evolution

of the microstructure, as accounted for by the changing aspect ratios, may lead to overall hardening, or softening for the composite, as we will see in the next section.

4. APPLICATION TO AXISYMMETRIC LOADING CONDITIONS

In this section, we consider the application of the above constitutive model to the finite axisymmetric deformation of a two-phase rigid–perfectly plastic composite with particulate microstructure. Because of the incompressibility of the constituent phases, the volume fractions of the inclusion and matrix phases, $c^{(1)}$ and $c^{(2)}$, respectively, remain fixed during the deformation process. In addition, it suffices to specify the axial strain rate $\bar{D}_{33}$, taken to be constant, in such a way that $\bar{D}_{11} = \bar{D}_{22} = -\frac{1}{2}\bar{D}_{33}$ are also constant. On the other hand, the stress components $\bar{\sigma}_{33}$ and $\bar{\sigma}_{11} = \bar{\sigma}_{22}$ are indeterminate up to a hydrostatic pressure, which for convenience will be taken such that $\bar{\sigma}_{11} = \bar{\sigma}_{22} = 0$. All other components of the strain rate and stress tensors are also zero.

For the case of uniform axial strain rate, the axial logarithmic strain is obtained by integration with respect to time (t), which gives

$$\bar{\varepsilon}_{33} = \bar{D}_{33} t, \tag{21}$$

so that $\bar{\varepsilon}_{33}$ may be taken to be a time-like variable. Further, due to the symmetry of the loading, in this case, the two aspect ratios from eqns (5) are identical, $w_1 = w_2 = w$, so that w satisfies the relation

$$\dot{w} = \tfrac{3}{2} w D_{33}^{(1)} = \tfrac{9}{4} w A_{3333}^{(1)} \bar{D}_{33}. \tag{22}$$

Before proceeding with the application of the model to the rigid–perfectly plastic composite, we first show an application to a linearly viscous composite, for the purpose of highlighting the differences in the evolution problem for the linear and nonlinear composites. The evolution of the aspect ratio for an isolated inclusion has been considered by Bilby *et al.* (1975). Next, we carry out analogous analyses for composites with nondilute concentrations of inclusions, exploring the effects of evolving microstructure on the effective stress–strain rate relations.

4.1. *Linearly viscous composites*

The inclusion and matrix phases are taken to be incompressible with viscosities $\mu^{(1)}$ and $\mu^{(2)}$. Then, relation (7) may be used to solve for the axial stress $\bar{\sigma}_{33}$ in terms of the given, constant axial component of the strain rate $\bar{D}_{33}$. The result is

$$\bar{\sigma}_{33} = 3\tilde{\mu}_{\mathrm{d}} \bar{D}_{33}, \tag{23}$$

where $\tilde{\mu}_{\mathrm{d}}$ is the effective shear stress for the axisymmetric mode, given eqns (A4) of Part I, in terms of $\mu^{(2)}$, the viscosity ratio $y^{(1)}$, the proportions of the phases $c^{(1)}$ and $c^{(2)}$, and the aspect ratio of the inclusions w. All of these variables are constant throughout the deformation process, except w, which evolves in time according to eqn (22). Noting that

$$A_{3333}^{(1)} = \frac{4(w^2-1)}{6(w^2-1) - 9c^{(2)}(y^{(2)}-1)(h - 2w^2 + 2hw^2)}, \tag{24}$$

where $h = h(w)$ is given by eqn (A5) of Part I, and assuming that the microstructure is initially isotropic (i.e. spherical inclusions), we obtain the following expression for w by

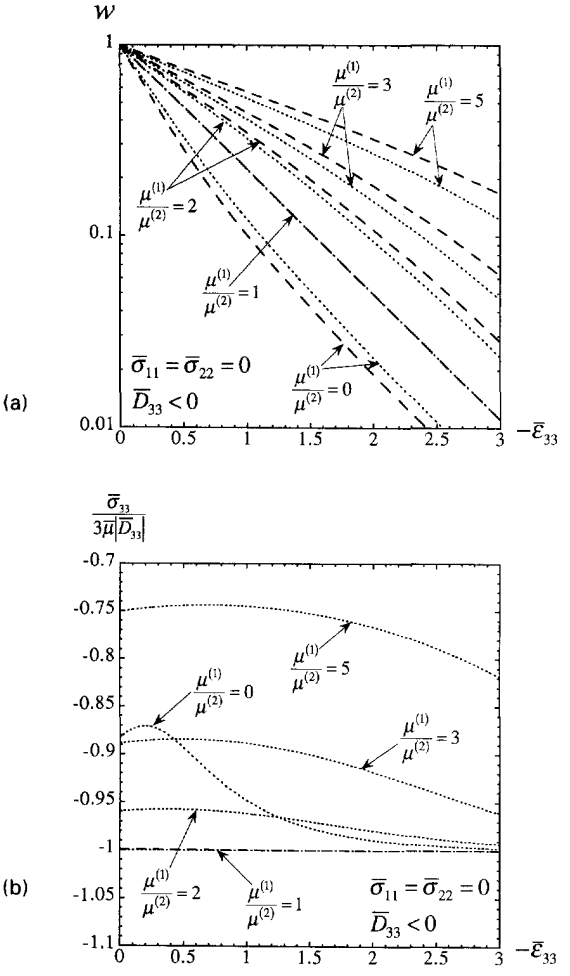

Fig. 1. Application of the model to uniaxial compression of two-phase linearly viscous composite with initially isotropic distribution of spherical inclusions ($w = 1$), for different values of the viscosity ratio $y^{(2)}$. The dashed and dotted lines correspond to dilute and finite concentrations of inclusions ($c^{(1)} = 0.001$ and 0.2). (a) Evolution of the aspect ratio w. (b) Evolution of the compressive stress $\bar{\sigma}_{33}$.

integration of eqn (22):

$$\bar{\varepsilon}_{33} = \begin{cases} \frac{2}{3}\ln(w) + c^{(2)}(y^{(2)}-1)\left[\frac{1}{3} + \frac{1-w(w^2-1)^{-1/2}\cosh^{-1}(w)}{w^2-1}\right] & \text{if} \quad w > 1, \\ \frac{2}{3}\ln(w) + c^{(2)}(y^{(2)}-1)\left[\frac{1}{3} - \frac{1-w(1-w^2)^{-1/2}\cos^{-1}(w)}{1-w^2}\right] & \text{if} \quad w < 1. \end{cases} \tag{25}$$

We note that this expression generalizes a corresponding expression by Bilby *et al.* (1975) for the isolated inclusion problem (the same expression with $c^{(2)}$ replaced by 1).

Finally, putting this implicit result for w as a function of $\bar{\varepsilon}_{33}$ together with eqn (23), we are able to compute the axial stress $\bar{\sigma}_{33}$ as a function of $\bar{\varepsilon}_{33}$. Figures 1(a) and (b) give the evolution of w and $\bar{\sigma}_{33}$, respectively, as functions of $\bar{\varepsilon}_{33}$ (time) for a compressive deformation history ($\bar{D}_{33} < 0$). Two values are chosen for the volume fractions of the inclusion phase $c^{(1)}$, one in the dilute range and one in the nondilute range (0.001 and 0.2), and several viscosity ratios $y^{(2)}$ are also chosen (0, 1, 2, 3, 5). It is observed in Fig. 1(a) that w decreases under compressive conditions, with w decreasing faster for the composites with the weaker inclusions than for the composites with the stronger inclusions. Also, it is

observed that the composites with finite concentration of inclusions exhibit the same trends for w as the composites with dilute concentrations of inclusions, except that the effect of the viscosity ratio is less marked for the composites with finite concentrations of inclusions. Figure 1(b) shows plots of the evolution of $\bar{\sigma}_{33}$, normalized by $\bar{\mu}|\bar{D}_{33}|$. When the viscosity ratio is unity, or for dilute concentrations of inclusions, the plot is a straight line with zero slope, indicating a linear relationship between $\bar{\sigma}_{33}$ and $\bar{D}_{33}$, as expected for a homogeneous linearly viscous material. However, it is clear from Fig. 1(b) that the evolution of the shape of the inclusions, when present in finite volume fractions, leads to a nonlinear response. The strength of the nonlinearity increases as the viscosity ratio increases, or decreases from unity. The reason for the enhanced nonlinear behavior with increasing, or decreasing, viscosity ratio may be attributed to the fact that the limiting shapes for the inclusions are flat layers. Since the effective viscosity of a laminated microstructure, under this loading mode, is precisely the arithmetic (Voigt) average of the viscosities of the two phases (i.e. $\bar{\mu}$), this means that the effective viscosity of the composites with the initially spherical inclusions, which is strictly smaller in magnitude than the arithmetic average of the viscosities, will have to change toward the Voigt average as the shape of the inclusions changes toward the flat layer limit. This is precisely what is observed in Fig. 1(b). However, the changes are faster for the weaker inclusions, because the weaker inclusions deform more quickly than the stronger ones [see Fig. 1(a)].

Figures 2(a) and (b) give the corresponding plots for the evolution of w and $\bar{\sigma}_{33}$ for a tensile deformation history ($\bar{D}_{33} > 0$). The same values of $c^{(1)}$ and $y^{(2)}$ are chosen as in Fig. 1. It is observed in Fig. 2(a) that w increases for tensile conditions, with w increasing faster for the composites with the weaker inclusions. It is also seen from this figure that the composites with finite concentration of inclusions exhibit the same trends for w as the composites with dilute concentrations of inclusions, except that the effect of the viscosity ratio is less marked for the composites with finite concentrations of inclusions. Figure 2(b) shows plots of the evolution of $\bar{\sigma}_{33}$, normalized by $\bar{\mu}|\bar{D}_{33}|$. Once again, it is seen that the presence of inhomogeneities, in finite concentration, leads to a nonlinear relation between $\bar{\sigma}_{33}$ and $\bar{D}_{33}$. The strength of the nonlinearity increases as the viscosity ratio increases or decreases from unity. The reason for this is that the limiting shapes for the inclusions are infinite fibers. Since the effective viscosity of aligned fiber microstructures is also the arithmetic average of the viscosities of the two phases ($\bar{\mu}$), this means that the effective viscosity of the composites with the initially spherical inclusions, which is strictly below the arithmetic average of the viscosities of the two phases, will have to climb toward the Voigt average as the shape of the inclusions changes toward the infinite fiber limit. Less viscous inclusions will change more quickly, but the changes will be smaller in relative terms.

4.2. *Rigid–perfectly plastic composites*

The inclusion and matrix phases are taken to be incompressible with yield strengths $\sigma_y^{(1)}$ and $\sigma_y^{(2)}$, respectively. Because the state of stress is uniaxial, the yield condition (17) specializes in this case to

$$\bar{\sigma}_{33} = \sqrt{3}\tilde{\tau}_d, \tag{26}$$

where $\tilde{\tau}_d$ is the effective yield stress in the axisymmetric mode, determined by an equation completely analogous to eqn (25) of Part I, namely,

$$\left(\frac{\tilde{\tau}_d}{\tau_y^{(2)}}\right)^2 = \min_{y^{(1)} \geq 0} \left\{ [c^{(2)} + c^{(1)}(z^{(2)})^2 y^{(1)}] \left[\frac{g_3^{(2)} y^{(1)} + g_4^{(2)}}{g_1^{(2)} y^{(1)} + g_2^{(2)}} \right] \right\}, \tag{27}$$

where the $g_i^{(2)}$ are given by eqns (A4) of Part I. Note that this expression depends on the matrix yield strength $\sigma_y^{(2)}$, the yield strength ratio $z^{(2)}$, the proportions of the phases $c^{(1)}$ and $c^{(2)}$, and the aspect ratio of the inclusions w. Of all these variables, only w changes during the deformation history, so that the axial stress $\bar{\sigma}_{33}$ will also vary in a way determined by the changes in w.

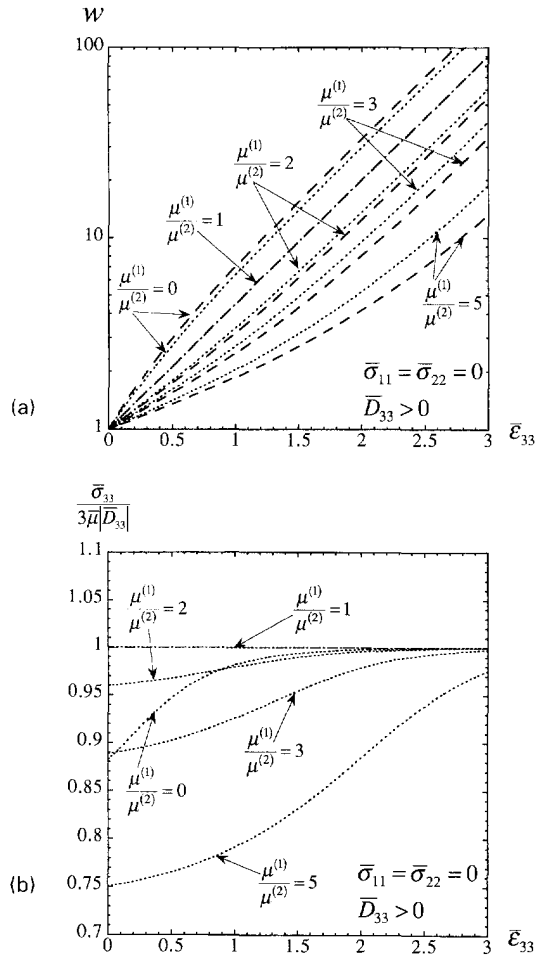

Fig. 2. Application of the model to uniaxial tension of two-phase linearly viscous composite with initially isotropic distribution of spherical inclusions ($w = 1$), for different values of the viscosity ratio $\hat{\mu}^{(2)}$. The dashed and dotted lines correspond to dilute and finite concentrations of inclusions ($c^{(1)} = 0.001$ and 0.2). (a) Evolution of the aspect ratio w. (b) Evolution of the tensile stress $\bar{\sigma}_{33}$.

To determine the evolution of w, we require the corresponding expression for $A^{(1)}_{3333}$ in eqn (22); it is given by

$$A^{(1)}_{3333} = \frac{4(w^2-1)}{6(w^2-1)-9c^{(2)}(\hat{\gamma}^{(2)}-1)(h-2w^2+2hw^2)}, \tag{28}$$

where $\hat{\gamma}^{(2)} = (\hat{\gamma}^{(1)})^{-1}$ is obtained from the optimization problem in eqn (27), and $h = h(w)$ [the explicit expressions are given by eqn (26), with the $e_i^{(2)}$ replaced by $g_i^{(2)}$, and (A5), respectively, of Part I]. Unfortunately, due to the complicated dependence of $\hat{\gamma}^{(2)}$ on w, the integration of eqn (22) for w must be carried out numerically. Nevertheless, once the history of w is known for given yield stress ratios and volume fractions, the corresponding history of the axial stress $\bar{\sigma}_{33}$ may be determined from eqn (26) with (27). In addition, we may compute the effective hardening rate H from relation (20); however, the effective constitutive relations (19) are not needed in this simple example (we could simply verify that they are satisfied).

Before going on to the presentation of the results of this analysis for some specific values of the volume fractions and yield strengths, we recall from Part I that when the matrix is weaker than the inclusions, and ratio $z^{(2)}$ exceeds a certain critical value, $z_d^{(2)}$, depending on w [see Fig. 4(c) of Part I], the inclusions behave as rigid particles, and further increases in the yield strength of the inclusions do not result in additional increases in

the effective strength of the composite. Indeed, this feature of the rigid–perfectly plastic composites was identified with the fact that $\hat{y}^{(1)} = 0$ for $z^{(2)} \geqslant z_d^{(2)}$. We are now in a position to verify, from eqn (28), that the inclusion strain concentration does indeed vanish, for given w, when $z^{(2)} \geqslant z_d^{(2)}$. In the context of the evolution problem, this implies that, if during a deformation history, the particle attains a shape (w) for which $z^{(2)}$ is in excess of $z_d^{(2)}$, then the particle will abruptly stop changing shape. In particular, if the particle initially has a shape for which $z^{(2)}$ is greater than $z_d^{(2)}$, the particle will remain frozen in shape, and therefore the stress will also remain constant. Note that for spherical particles with $c^{(1)} = 0.2$, $z_d^{(1)} = 0.456$.

In Figs 3 and 4, we give plots of w, $\bar{\sigma}_{33}$ and H as functions of $\bar{\varepsilon}_{33}$ for $c^{(1)} = 0.2$, and several values of the yield strength ratio $z^{(1)}$ (0.47, 0.5, 0.6 and 0.7, 1, 2, 5), such that the inclusions are harder (softer) than the matrix for values of $z^{(1)}$ less (greater) than unity. Figure 3 gives results for a compressive deformation history ($\bar{D}_{33} < 0$) and Fig. 4 gives the corresponding results for a tensile deformation history ($\bar{D}_{33} > 0$).

In Fig. 3(a), we observe that w for the initially spherical inclusions decreases with increasing compressive deformation. This decrease is more marked for the relatively weaker inclusions (higher values of $z^{(1)}$). On the other hand, for $z^{(1)} = 0.47$, we find that the inclusions change shape only slightly (from $w = 1$ to 0.865) before locking up at a relatively small strain. This may be understood in the terms discussed above: Fig. 4(c) of Part I shows that $z^{(1)} = 0.47$ is in the deformable region of the plot for $w = 1$, but a small decrease in w leads to a sufficient increase in $z_d^{(1)}$ to reach the condition $z^{(1)} = z_d^{(1)}$, resulting in rigid behavior for the inclusion.

Figure 3(b) shows the corresponding plots for $\bar{\sigma}_{33}$, normalized relative to the arithmetic average of the yield strengths of the two phases [the so-called upper bound of Bishop and Hill (1951)]. For inclusions stronger than the matrix ($z^{(1)} = 0.5$–0.7), $\bar{\sigma}_{33}$ initially decreases in magnitude, to then reverse its trend, and increase toward the Bishop–Hill bound. The fact that the stress should initially decrease in magnitude may be understood from Fig. 4(a) of Part I, which shows that the effective yield strength of a composite with stronger inclusions (HS−) in the axisymmetric mode has its minimum for a value of w somewhat less than 1 (about 0.6). This means that the composite with w decreasing from 1 will actually weaken until w reaches some value less than 1, after which point the composite will begin to strengthen again. The fact that the effective yield strength of the composite in this mode will approach the Bishop–Hill upper bound for the strength is a consequence of the fact that the limiting shape for the inclusions is that of layers, corresponding to a laminated composite with effective yield strength in the axisymmetric mode equal to the arithmetic average of the phases [see Ponte Castañeda and deBotton (1992) and Part I]. In addition, we observe, in agreement with the discussion in the previous paragraph, that $\bar{\sigma}_{33}$ for the composite with $z^{(1)} = 0.47$ decreases in magnitude slightly until the critical condition is met and the inclusions no longer deform. Once this happens, the hardening mechanism induced by the decreasing w is switched off, and $\bar{\sigma}_{33}$ remains constant for the rest of the deformation history. Finally, for weaker inclusions ($z^{(1)} = 2, 5$), the same qualitative behavior is observed as for stronger inclusions, although the changes are smaller in magnitude, but they take place over a shorter time scale. Also, the lock up phenomenon was not observed for weaker inclusions [that this should be the case can be seen from Fig. 4(c) of Part I].

Figure 3(c) gives the corresponding plots for the effective hardening rates. These are in agreement with the remarks in the previous paragraphs for the stresses. For all shown values of $z^{(1)}$ (except 0.47), H is initially negative due to the initial weakening of the composite, but then becomes positive at a relatively small strain to then tend to zero for large strain. On the other hand, H is initially negative for the composite with $z^{(1)} = 0.47$ until the inclusions become effectively rigid, when H becomes zero. The fact that H is initially negative for these composites indicates that these materials may tend to be initially unstable under compressive axisymmetric deformations. However, for sufficiently large compressive deformations, the deformation should stabilize due to the continuing change in shape of the inclusions.

In Fig. 4(a), we observe that the w of the initially spherical inclusions increases for this class of tensile deformation history. This increase is more marked for the relatively weaker

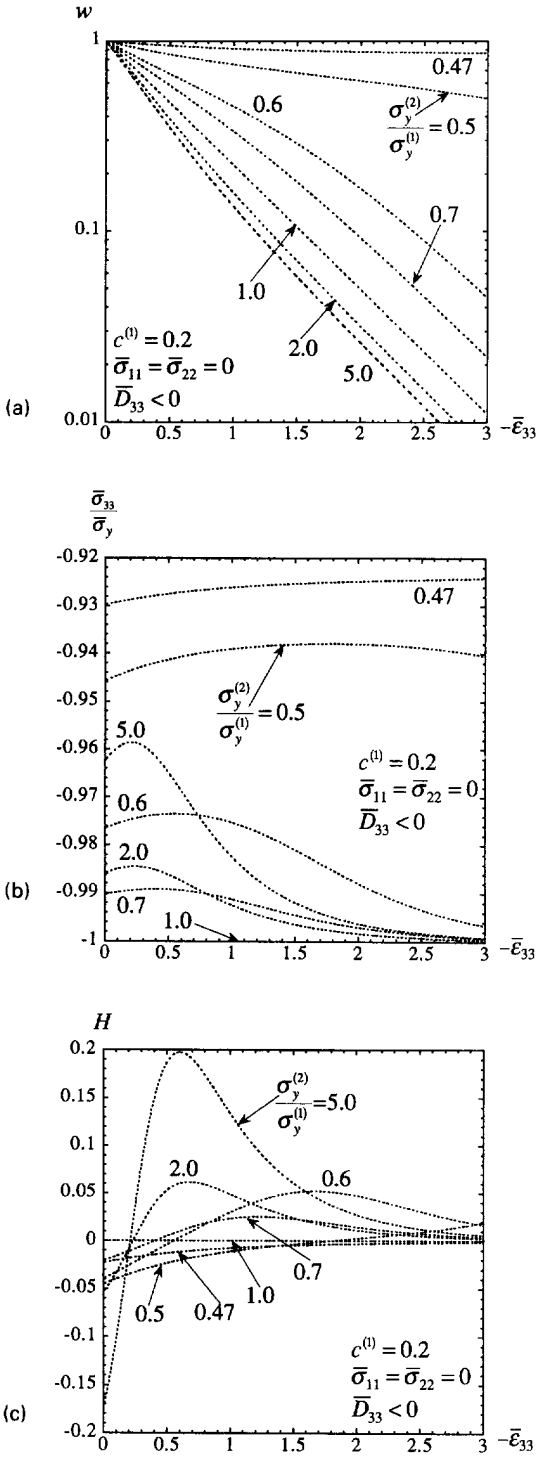

Fig. 3. Application of the model to uniaxial compression of two-phase rigid–perfectly plastic composite with initially isotropic distribution of spherical inclusions ($w = 1$), for different values of the yield strength ratio $z^{(1)} = \sigma_y^{(2)}/\sigma_y^{(1)}$. (a) Evolution of the aspect ratio w. (b) Evolution of the compressive stress $\bar{\sigma}_{33}$. (c) Evolution of the effective hardening rate H.

inclusions (higher values of $z^{(1)}$). However, there is no "lock up" phenomenon in this case, even for relatively small values of $z^{(1)}$. Of course, for small enough values of $z^{(1)}$, the inclusions will remain frozen in their original shapes ($w = 1$). These results may be checked against Fig. 4(c) of Part I, which shows that, with w increasing from unity, either the

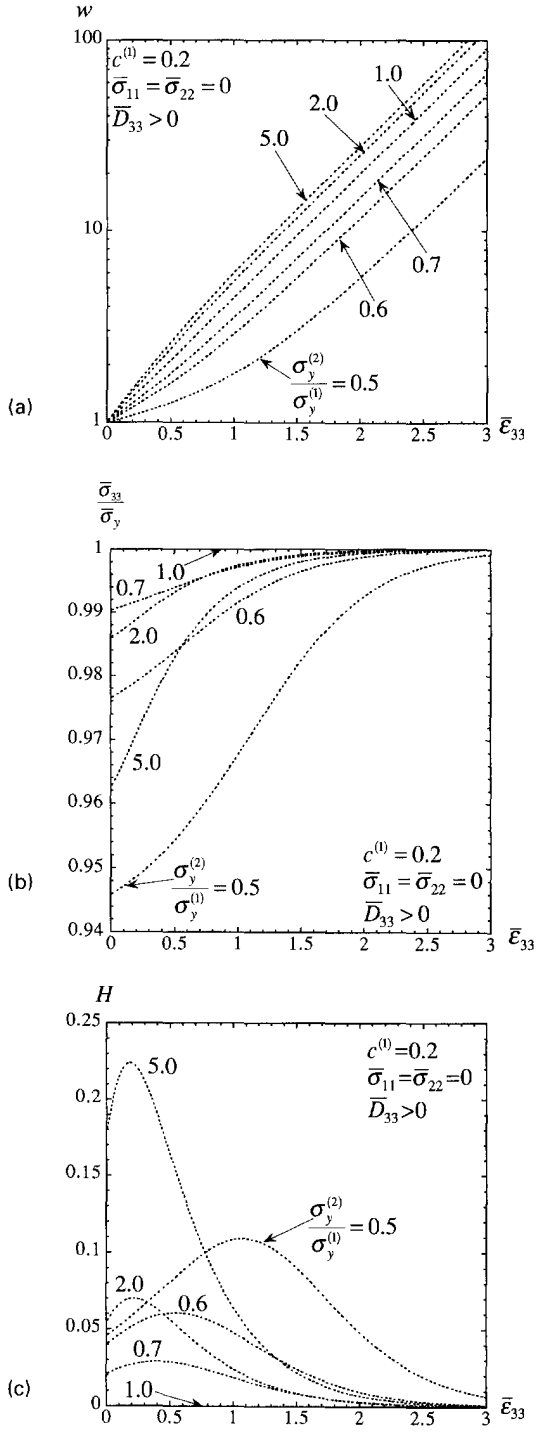

Fig. 4. Application of the model to uniaxial tension of two-phase rigid–perfectly plastic composite with initially isotropic distribution of spherical inclusions ($w = 1$), for different values of the yield strength ratio $z^{(1)} = \sigma_y^{(2)}/\sigma_y^{(1)}$. (a) Evolution of the aspect ratio w. (b) Evolution of the tensile stress $\bar{\sigma}_{33}$. (c) Evolution of the effective hardening rate H.

inclusions will deform unhindered to their asymptotic shape of fibers, or they will not deform at all.

In Fig. 4(b), we show the corresponding plots for $\bar{\sigma}_{33}$, normalized relative to the Bishop–Hill average. For this case involving uniaxial tension, $\bar{\sigma}_{33}$ increases monotonously

toward the higher Bishop–Hill (arithmetic) average stress. The increase in $\bar{\sigma}_{33}$ is relatively more significant for the smaller values of $z^{(1)}$ (stronger inclusions). However, the weaker inclusions deform faster than the stronger ones, as a consequence of the faster changes in aspect ratio. The fact that $\bar{\sigma}_{33}$ approaches the Bishop–Hill average is a consequence of the fact that the axisymmetric yield strength of a fiber-reinforced composite is precisely the arithmetic average of the yield strength of the phases [see Ponte Castañeda and deBotton (1992) and Part I].

Figure 4(c) gives the corresponding plots for the effective hardening rates. These are in agreement with the remarks in the previous paragraphs for the stresses. For the values of $z^{(1)}$ shown in the plot, H is positive throughout the deformation history, but it tends to zero for large enough strains. This result has the physical interpretation that the evolution of the shape of the inclusions has a stabilizing effect on the deformation.

5. APPLICATION TO PLANE STRAIN LOADING CONDITIONS

In this section, we consider the application of the constitutive model to the finite deformation of a two-phase rigid–perfectly plastic composite under plane strain conditions. We note that Howard and Brierley (1976) [see also Bilby *et al.* (1975)] determined the change in shape of an isolated linearly viscous inclusion in a linearly viscous matrix phase. Letting x_2 denote the constrained direction, so that $\bar{D}_{22} = 0$, and imposing in-plane uniaxial tension, such that $\bar{D}_{33} \neq 0$ and $\bar{\sigma}_{11} = 0$, it remains to determine the nonzero stresses $\bar{\sigma}_{22}$ and $\bar{\sigma}_{33}$ and aspect ratios w_1 and w_2, as functions of the logarithmic strain $\bar{\varepsilon}_{33} = \bar{D}_{33}t$.

In terms of the optimal $\hat{y}^{(1)}$ from relation (17), $\bar{D}_{22} = 0$ and relation (19) imply that

$$\bar{\sigma}_{22} = -\frac{\tilde{m}_{2233}(\hat{y}^{(1)})}{\tilde{m}_{2222}(\hat{y}^{(1)})}\bar{\sigma}_{33}. \tag{29}$$

It then follows from eqn (17) that

$$\bar{\sigma}_{33}^2 = [c^{(1)}\hat{y}^{(1)}(z^{(2)})^2 + c^{(2)}]\left[\tilde{m}_{3333}(\hat{y}^{(1)}) - \frac{(\tilde{m}_{2233}(\hat{y}^{(1)}))^2}{\tilde{m}_{2222}(\hat{y}^{(1)})}\right]^{-1}(\sigma_y^{(2)})^2. \tag{30}$$

The evolution of the aspect ratios is obtained from expressions (5), with $\mathbf{A}^{(1)} = \mathbf{A}^{(1)}(\hat{y}^{(1)}; w_1, w_2)$ obtained from expression (2), in terms of the Eshelby tensor $\mathbf{S}^{(2)}$ for a general ellipsoidal inclusion (which is computed numerically). Once this is done, $\bar{\sigma}_{22}$ and $\bar{\sigma}_{33}$ may be computed from eqns (29) and (30). Solutions with a compressive strain rate in the axial direction ($\bar{D}_{33} < 0$) for a composite material with volume fractions $c^{(1)} = c^{(2)} = 0.5$, initial aspect ratios $w_1 = w_2 = 1$ and contrast ratios $\sigma_y^{(1)}/\sigma_y^{(2)} = 0.5, 0.6, 0.7$ are plotted in Fig. 5. Recall that the inclusion and matrix phases are denoted by 1 and 2, respectively, so that with the above choices of contrast ratios, the matrix is always stronger than the inclusions. The plots depict the evolution of the aspect ratios w_1, w_2, the nonzero stresses $\bar{\sigma}_{22}$, $\bar{\sigma}_{33}$ and the hardening rate coefficient H, all as functions of the average axial strain $\bar{\varepsilon}_{33}$.

It is observed, from Fig. 5(a), that the aspect ratios of the inclusions decrease, under compression, faster in the unconstrained direction x_1 than in the direction in which the applied strains are constrained to vanish (the x_2 direction). Thus, the initially spherical inclusions become shorter in the x_3 direction and longer in the x_1 direction. Looking at Fig. 5(b) and (c), we observe that the material hardens initially in both the x_2 and x_3 directions, but as the deformation progresses, the material eventually softens in the x_2 direction. The overall response, however, is one of hardening, as may be observed in Fig. 5(d), where the hardening rate coefficient H is plotted and found to be always positive. Results were also computed for materials with inclusions stronger than the matrix [see Zaidman (1994)]. The findings are similar to those presented in this section except that the possibility of shape lock up is available in this case.

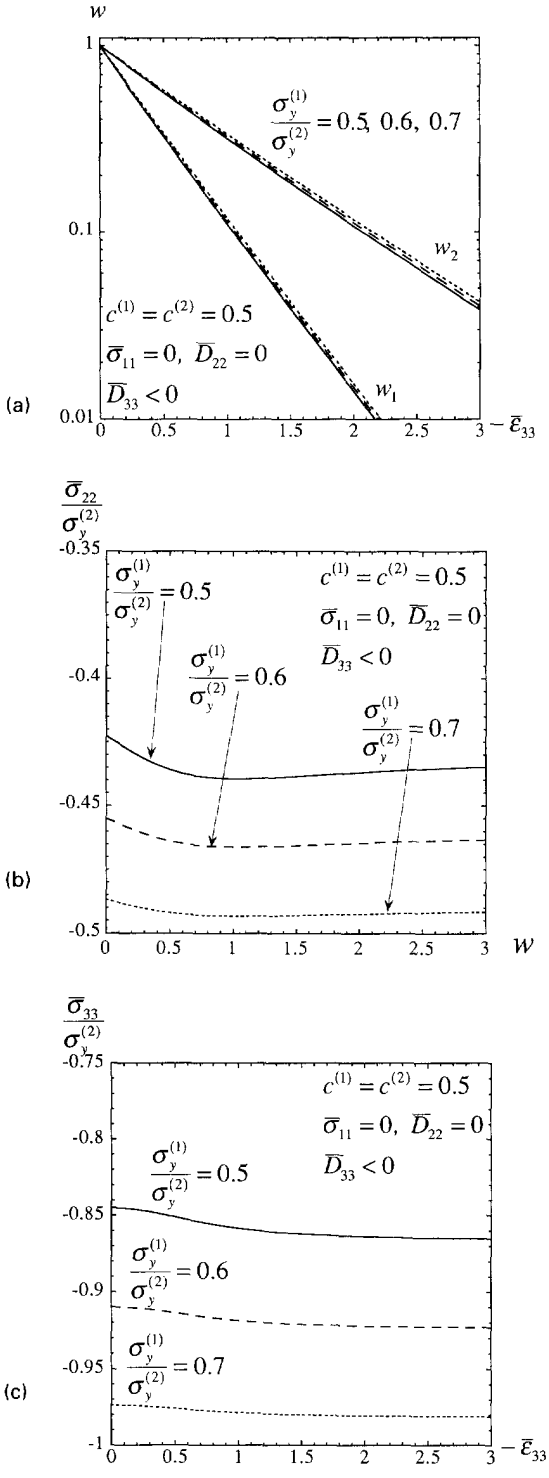

Fig. 5. Application of the model to plane strain compression ($\bar{D}_{22} = 0$, $\bar{D}_{33} < 0$, $\bar{\sigma}_{11} = 0$) of two-phase rigid–perfectly plastic composite with initially isotropic distribution of spherical inclusions ($w_1 = w_2 = 1$), for different values of the yield strength ratio $z^{(2)} = \sigma_y^{(1)}/\sigma_y^{(2)}$. (a) Evolution of the aspect ratios w_1 and w_2. (b) Evolution of the stress $\bar{\sigma}_{22}$. (c) Evolution of the stress $\bar{\sigma}_{33}$. (d) Evolution of the effective hardening rate H. (*Continued overleaf.*)

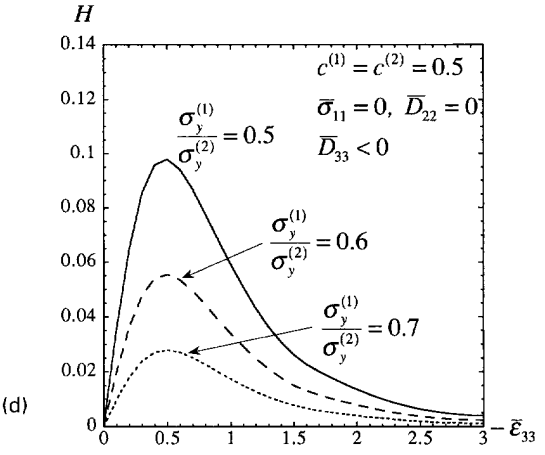

Fig. 5. (*Continued.*)

We finally remark that the hardening/softening induced by the change in the shape of the inclusions might be crucial in stability predictions for composite materials. For example, for plane strain loading conditions, the possibility of localization may be identified with the vanishing of the effective hardening rate H (Rice, 1976). This condition, which was not satisfied during the process described in Fig. 5, was found to be satisfied, in some cases, for initially anisotropic microstructures (Zaidman, 1994).

6. CONCLUDING REMARKS

In this work, we have developed a relatively simple constitutive model for two-phase nonlinear composites which is capable of accounting approximately for the evolution of the microstructure under finite deformation conditions. The constitutive model is made up of two parts: the instantaneous effective stress–strain rate relations and evolution equations for appropriate state variables serving to characterize the changes in the microstructure. Effective potentials and yield functions were obtained in Part I of the work for the class of particulate microstructures with ellipsoidal symmetry (corresponding to composites with distributions of aligned ellipsoidal inclusions). These potentials and yield functions are valid for general loading conditions and for arbitrary values of the phase concentrations and inclusion aspect ratios. Evolution equations were proposed in this part for the phase concentrations and aspect ratios, for conditions of general triaxial loading, aligned with the symmetry axes of the composite materials. Explicit computations were carried out for two-phase linearly viscous and rigid–perfectly plastic composites subjected to axisymmetric and plane strain loading conditions. The main finding is that—due to the evolution of the microstructure—the effective behavior of the composite may be qualitatively different from that of the constituent phases. Thus, we found that the effective response of a composite with linearly viscous phases is nonlinearly viscous, whereas the effective response of a composite with perfectly plastic phases may exhibit hardening, or even softening, depending rather strongly on the specific loading conditions.

These findings may have significant implications in metal forming processes, where success is often measured by the prevention of the development of shear bands and other instabilities (e.g. forming limits). It is know from the work of Rice (1976) that shear bands may develop in rigid–plastic materials when the hardening rate vanishes, provided a certain kinematical condition is satisfied. In the analysis of Section 4, for homogeneous axisymmetric loading of composites with rigid–perfectly plastic phases, it was found that the effective hardening rate could become zero under compressive loading. (Note that adding slight hardening to the phases would not be expected to change the qualitative features of the effective hardening curves.) However, because of the special nature of axisymmetric

deformations, the kinematical condition was not met, and therefore the possibility of shear localization could be excluded in this case. Nevertheless, the principle that the presence of inhomogeneities in the finite deformation of a rigid–plastic material may affect the effective hardening rate of the material, in such a way as to affect the possible development of shear bands, was established. Conversely, one could also envisage the "intelligent" use of inhomogeneities in a material—to enhance the effective hardening rate of the material—as a tool to control the development of shear bands and other instabilities in forming processes. Thus, we saw, in the examples of Section 4, that the effective hardening rate of the composite was always positive under tensile conditions, even though the phases themselves exhibited perfectly plastic behavior. This enhancement in the effective hardening of the composite would be expected to make the material more stable during the given deformation process.

Acknowledgements—This work was supported by NSF grant MSS-92-02513 and by the NSF/MRL Program at the University of Pennsylvania under grant no. DMR91-20668. This manuscript was completed while one of the authors (P.P.C.) was a Visiting Professor at the Laboratoire de Mecanique des Solides, Ecole Polytechnique, Paris. Thanks are due to Mahesh Kailasam for useful comments on an earlier version of this manuscript.

REFERENCES

Bilby, B. A. and Kolbuszewski, M. L. (1977). The finite deformation of an inhomogeneity in two-dimensional slow viscous incompressible flow. *Proc. R. Soc. Lond. A* **355,** 335–353.

Bilby, B. A., Eshelby, J. D. and Kundu, A. K. (1975). Change in shape of a viscous ellipsoidal region embedded in a slowly deforming matrix having a different viscosity. *Techtonophysics* **28,** 265–274.

Bishop, J. F. W. and Hill, R. (1951). A theory of the plastic distorsion of a polycrystalline aggregate under combined stresses. *Phil. Mag.* **42,** 414–427.

Eshelby, J. D. (1957). The determination of the elastic field of an ellipsoidal inclusion, and related problems. *Proc. R. Soc. Lond. A* **241,** 376–396.

Hashin, Z. and Shtrikman, S. (1963). A variational approach to the theory of the elastic behavior of multiphase materials. *J. Mech. Phys. Solids* **11,** 127–140.

Hill, R. (1965). Continuum micromechanics of elastoplastic polycrystals. *J. Mech. Phys. Solids* **13,** 89–101.

Howard, I. C. and Brierley, P. (1976). On the finite deformation of an inhomogeneity in a viscous liquid. *Int. J. Engng Sci.* **14,** 1151–1159.

Ponte Castañeda, P. (1991). The effective mechanical properties of nonlinear isotropic solids. *J. Mech. Phys. Solids* **39,** 45–71.

Ponte Castañeda, P. (1992). New variational principles in plasticity and their application to composite materials. *J. Mech. Phys. Solids* **40,** 1757–1788.

Ponte Castañeda, P. and deBotton, G. (1992). On the homogenized yield strength of two-phase composites. *Proc. R. Soc. Lond. A* **438,** 419–431.

Ponte Castañeda, P. and Zaidman, M. (1994). Constitutive models for porous materials with evolving microstructure. *J. Mech. Phys. Solids* **42,** 1459–1497.

Ponte Castañeda, P. and Zaidman, M. (1996). The finite deformation of nonlinear composite materials—I. Instantaneous constitutive relations. *Int. J. Solids Structures* **33,** 1271–1286.

Rice, J. R. (1976). The localization of plastic deformation. In *Proceedings of the 14th International Congress of Theoretical and Applied Mechanics* (Edited by W. T. Koiter), p. 20. North-Holland, Amsterdam.

Willis, J. R. (1977). Bounds and self-consistent estimates for the overall moduli of anisotropic composites. *J. Mech. Phys. Solids* **25,** 185–202.

Willis, J. R. (1978). Variational principles and bounds for the overall properties of composites. In *Continuum Models for Discrete Systems* (Edited by J. W. Provan), pp. 185–215. University of Waterloo Press.

Zaidman, M. (1994). Composite materials with evolving microstructures. Ph.D. Thesis, Department of Mechanical Engineering and Applied Mechanics, University of Pennsylvania.